HHS Public Access

Author manuscript

Acta Biomater. Author manuscript; available in PMC 2022 August 01.

Published in final edited form as:

Acta Biomater. 2021 August ; 130: 281–290. doi:10.1016/j.actbio.2021.06.007.

Human Neutrophil FcγRIIIb Regulates Neutrophil Extracellular Trap Release in Response to Electrospun Polydioxanone Biomaterials

Allison E. Fetz[a], **Marko Z. Radic**[b], **Gary L. Bowlin**[a]

[a]Department of Biomedical Engineering, University of Memphis, 3806 Norriswood Avenue, Memphis, TN, USA

[b]Department of Microbiology, Immunology, and Biochemistry, College of Medicine, University of Tennessee Health Science Center, 858 Madison Avenue, Memphis, TN, USA

Abstract

During the acute inflammatory response, the release of neutrophil extracellular traps (NETs) is a pro-inflammatory, preconditioning event on a biomaterial surface. Therefore, regulation of NET release through biomaterial design is one strategy to enhance biomaterial-guided *in situ* tissue regeneration. In this study, IgG adsorption on electrospun polydioxanone biomaterials with differing fiber sizes was explored as a regulator of *in vitro* human neutrophil NET release. The propensity to release NETs was increased and decreased by modulating adsorbed IgG, suggesting a functional link between IgG and NET formation. Fiber-size dependent NET release was reduced by blocking FcγRIIIb, but not FcγRI, FcγRIIa, or Mac-1 (CD11b/CD18), indicating a specific receptor mediated neutrophil response. Inhibition of transforming growth factor-β-activated kinase 1 (TAK1), which is activated downstream of FcγRIIIb, significantly reduced the release of NETs in a fiber size-independent manner. These results indicate that *in vitro* electrospun biomaterial-induced NET release is largely regulated by IgG adsorption, engagement of FcγRIIIb, and signaling through TAK1. Modulation of this pathway may have beneficial therapeutic effects for regulating neutrophil-mediated inflammation by avoiding the adverse effects of NETs and increasing the potential for *in situ* tissue regeneration.

Graphical Abstract

Corresponding Author: Gary L. Bowlin, 330 Engineering Technology Building, 3806 Norriswood Avenue, Memphis, TN 38152, USA, glbowlin@memphis.edu, 901-678-2670.

Declaration of interests

The authors declare that they have no known competing financial interests or personal relationships that could have appeared to influence the work reported in this paper.

Disclosures: The authors have no conflicts of interest to disclose.

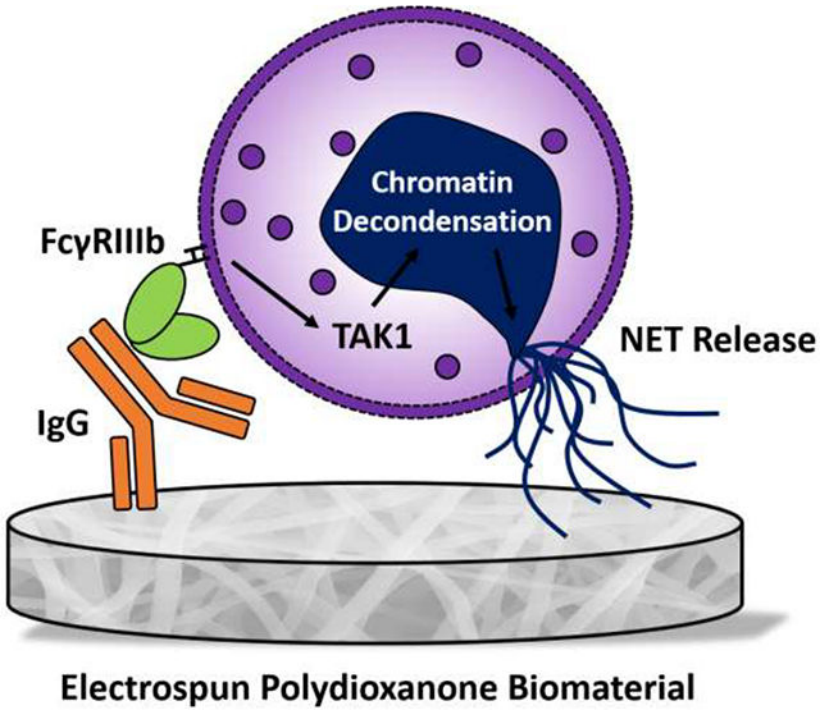

Keywords

neutrophils; biomaterials; electrospinning; neutrophil extracellular traps; tissue engineering

1. Introduction

For several decades, electrospun biomaterials have been used to create extracellular (ECM) analogs for a variety of tissue engineering applications [1–3]. Because electrospinning systems are relatively easy to build and adapt to large-scale production, electrospinning is a cost-effective fabrication technique for producing non-woven substrates of continuous fibers in large quantities. Furthermore, electrospun biomaterials offer vast versatility and adaptability for tissue engineering, including *in vitro* and *in situ* tissue regeneration. For *in situ* tissue regeneration, the purpose of the electrospun biomaterial is to guide the body as a bioreactor to stimulate the regenerative capacity of autologous cells, tissues, and organs [4]. Given the reliance on autologous cells to infiltrate the biomaterial, the inflammatory and immune response to the electrospun biomaterial are of utmost importance for biomaterial-guided *in situ* tissue regeneration [5].

In recent years, our group has focused on characterizing and understanding the neutrophil response to electrospun biomaterials [6–11]. Peaking in numbers near 24 to 48 hours after implantation, neutrophils are the first dynamic cell population recruited to an electrospun biomaterial [12]. Their rapid and abundant recruitment suggests an important role in preconditioning the inflammatory state of the local environment, which may have a long-term impact on the potential for tissue regeneration [13, 14]. At an inflammatory site,

neutrophils influence the tissue milieu through several effector functions, including the release of neutrophil extracellular traps (NETs) [15].

NETs are extracellular structures composed of chromatin filaments, histones, and proteolytic enzymes normally found within the cytoplasm and granules [15]. Although they are integral to pathogen containment [15–17], NETs can also be tissue destructive, resulting in prolonged inflammation and pathogenesis due to aberrant enzyme release and histone toxicity [18, 19]. In fact, NETs have been implicated in several non-infectious inflammatory diseases, such as autoimmune disorders, thrombosis, cancer, and tissue fibrosis [20–25]. Because of this, the potential deleterious effects of NETs have recently garnered attention in the field of biomaterials. Our group and others have shown that the release of NETs on the surface of a biomaterial is a significant preconditioning event that promotes inflammation and fibrosis [7, 26, 27]. In particular, we found that the fiber size of electrospun polydioxanone (PDO) regulates NET release with small fiber diameters (fiber diameter 0.4 ± 0.2 μm) significantly up-regulating NET release *in vitro* and *in vivo* and fibrotic encapsulation *in vivo* relative to large fiber diameters (fiber diameter 1.9 ± 0.7 μm). Together, these data suggest that one potential strategy to enhance biomaterial-guided *in situ* tissue regeneration is to regulate NET formation and its adverse effects through biomaterial design.

A variety of artificial and physiological stimuli have been shown to regulate NET release, including pharmacological compounds like phorbol 12-myristate 13-acetate (PMA) that act intracellularly and ligands that initiate outside-in signaling through various receptors [28–30]. Previously, we evaluated the adsorption of eight serum proteins on the surface of the electrospun PDO to begin elucidating the fiber size-dependent stimuli regulating NET formation on our biomaterials [31]. We found that nearly 2-times more IgG adsorbs to the surface of small fiber biomaterials compared to the large fiber biomaterials within 15 minutes when normalized to the mass of the biomaterials and that IgG adsorption was 100- to 200-times greater than any other protein, suggesting IgG signaling may increase the propensity to form NETs on small fibers. In fact, neutrophils constitutively express two fragment crystallizable gamma receptors (FcγR) for IgG, FcγRIIa (CD32a) and FcγRIIIb (CD16b) [32]. Both have been found to participate in the release of NETs stimulated by IgG immune complexes (ICs) [33–37]. Moreover, activated neutrophils express FcγRI (CD64) within 4–6 hours of activation [38–40], and Mac-1 (CD11b/CD18) can cooperate with FcγRs in the release of IC-induced NETs [34]. Given the prominent surface adsorption of IgG on our electrospun biomaterials, we hypothesize that IgG and FcγR signaling may be intimately linked to biomaterial-induced NET release.

In this work, we explored the role of IgG and FcγR signaling in electrospun biomaterial-induced NET release with human neutrophils. The propensity to release NETs was increased and decreased by increasing and decreasing adsorbed IgG, respectively, suggesting a functional link between IgG and NET formation. Then, blocking of FcγRIIIb, but not FcγRI, FcγRIIa, or Mac-1 (CD11b/CD18), resulted in a decrease in fiber-size dependent NET release, indicating a specific receptor mediated neutrophil response. Finally, incubation with 5Z-7-oxozeaenol, an inhibitor of FcγRIIIb signaling through transforming growth factor-β-activated kinase 1 (TAK1) [35], led to a decrease in NET formation on both

biomaterials. Together, these data show for the first time that surface adsorbed IgG, ligation of FcγRIIIb, and activation of TAK1 are involved in biomaterial-induced NET release. Our results indicate that regulation of IgG adsorption and FcγR signaling in neutrophils may be used to modulate NET release in biomaterial-guided tissue regeneration applications.

2. Materials and Methods

2.1 Electrospinning Biomaterials

Biomaterials were fabricated from PDO by electrospinning as previously described [31]. Briefly, PDO (Cat. No. 6100, Bezwada Biomedical, Hillsborough, NJ, USA) was dissolved overnight in 1,1,1,3,3,3-hexafluoro-2-propanol (Cat. No. 003409-1KG, Oakwood Products, Estill, SC, USA) at 50 and 120 mg/mL and electrospun with optimized parameters (Table 1) from a 5 mL syringe connected to an 18-gauge and 5 cm long blunt needle. Fibers were collected on a stainless steel, 100 mm long × 25 mm diameter cylindrical mandrel that was grounded and rotating at 1250 rpm while oscillating horizontally at 6.5 cm/s over 13 cm. For experiments, 8-mm diameter discs of the biomaterials, ranging in thickness from 0.05 to 0.10 mm, were cut using a biopsy punch (Cat. No. P825, Acuderm Inc., Fr. Lauderdale, FL, USA) and stored in a desiccator until use. Prior to cell culture, the biomaterials were disinfected by ultraviolet irradiation using an 8 W lamp (Cat. No. EN280L, Spectroline, Westbury, NY, USA) at a working distance of 9.5 cm. The samples were disinfected for 10 minutes on each side in a sterile, laminar flow hood and kept disinfected for cell culture.

2.2 Biomaterial Characterization

Scanning electron micrographs (SEMs) were acquired and analyzed in FibraQuant 1.3 software (nanoTemplate Technologies, LLC) to quantify fiber diameter as previously described [8]. Briefly, 150 semi-automated random measurements per SEM were taken to determine the average and corresponding standard deviation for fiber diameter.

2.3 Isolation and Culture of Primary Human Neutrophils

Heparinized, whole peripheral blood was obtained by venipuncture from unidentified, healthy donors from Tennessee Blood Services. Since purchased or donated samples are not traceable back to the donor, it does not qualify as human subjects research as determined by the University of Memphis Institutional Review Board on November 22, 2016. Neutrophils were then isolated by density separation as previously described [7, 8, 41]. Once isolated, neutrophils were resuspended in Hank's Balanced Salt Solution (HBSS) without calcium, magnesium, or phenol red (Cat. No. 14175095, Thermo Fisher Scientific, Waltham, MA, USA) and with 10 mM HEPES and 0.2% autologous serum at a concentration of 1 million neutrophils/mL. After placing the disinfected biomaterials (n = 4) in a 96-well plate, 40 μL of the cell culture media were added to each well to hydrate the biomaterials. For tissue culture plastic (TCP) wells (n = 4), 30 μL of the cell culture media were added prior to cell seeding. Subsequently, 100 μL of the cell suspension containing 100,000 neutrophils were added to each well. All wells then received 10 μL of heparin (Cat. No. H3393, Sigma Aldrich, St. Louis, MO, USA) at a final well concentration of 10 U/mL to dissociate NET-associated myeloperoxidase (MPO) as previously described [10, 17]. The positive and negative controls were TCP with 100 nM PMA (Cat. No. P8139, Sigma Aldrich, St. Louis,

MO, USA) and TCP with 0.15% dimethylsulfoxide (DMSO), respectively. The neutrophils were cultured on the biomaterials at 37°C and 5% CO_2 for 3 hours, and the TCP wells were cultured for 6 hours. Following culture, the samples were placed on ice for 10 minutes to inhibit neutrophil stimulation prior to fixing in 10% buffered formalin (Cat. No. SF1004, Thermo Fisher Scientific, Waltham, MA, USA) for 1 hour at room temperature. Three experiments were performed with unique donors (2 males, between 18 and 40 years of age, and 1 female, 25 years of age), and the results were pooled for analysis.

2.4 Addition of IgG to Biomaterials

To examine the dose-dependent effects of IgG on NET release, the biomaterials (n = 4) were hydrated with 1, 100, or 440 μg of human IgG (Cat. No. 31154, Thermo Fisher Scientific, Waltham, MA, USA) in 40 μL of HBSS for cell culture, equating to 0.025, 2.5, and 11 μg/μL, respectively. The mass of 1, 100, and 440 μg of IgG were selected to mimic the mass of IgG in 40 μL of cell culture media as the control, the mass of IgG needed to saturate the biomaterial surfaces, and the mass of IgG at physiological concentration, respectively. Controls were biomaterials hydrated with 40 μL of cell culture media.

2.5 Depletion of IgG from Biomaterials

To reduce the mass of surface-adsorbed IgG, IgG was depleted from autologous serum using Dynabeads™ Protein G (Cat. No. 10004D, Thermo Fisher Scientific, Waltham, MA, USA) [42]. Prior to use, Dynabeads™ Protein G were dialyzed in 12,000–14,000 molecular weight cutoff dialysis tubing in 1 L of phosphate buffered saline (PBS) for 48 hours at 4°C with gentle agitation. The PBS was refreshed every 12 hours. After dialysis, 100 μL of Dynabeads™ were added to the wells on a 96-well plate, placed on a handheld magnetic plate washer (Cat. No. NC1403679, Thermo Fisher Scientific, Waltham, MA, US), and washed five times with 250 μL of HBSS. Once the final wash was removed, 250 μL of 0.2% autologous serum in cell culture media was added to the Dynabeads™ and incubated for 30 minutes at room temperature with gentle agitation. Human IgG (Cat. No. 31154, Thermo Fisher Scientific, Waltham, MA, USA) diluted to a concentration of 0.2% in HBSS was used as an isotype control to validate the depletion. After incubation, the IgG-depleted supernatant was collected and sterile filtered with a 0.2 μM sterile filter. Subsequently, the biomaterials (n = 4) were hydrated with 40 μL of the IgG-depleted cell culture media prior to seeding the neutrophils. Controls were biomaterials hydrated with 40 μL of complete cell culture media containing 0.2% serum.

2.6 Validation of IgG Depletion

The depletion of IgG from autologous serum and the biomaterial surface was validated using immunodetection to quantify IgG as previously described [31]. Briefly, 30 μL of 0.2% autologous serum, IgG-depleted autologous serum, 0.2% isotype control IgG, and IgG-depleted isotype control (n = 3) were vacuum blotted on Immobilon-FL PVDF membrane (IPFL00005, EMD Millipore Corporation, Burlington, MA, USA) and dried overnight before processing and immunodetection. Free aldehyde groups on the fixed biomaterials were quenched with 100 mM glycine, and the PVDF membranes and biomaterials were then blocked and incubated with rabbit anti-IgG (ab109489, Abcam, Cambridge, MA, USA) followed by IRDye 800CW goat anti-rabbit (Part No. 925-32211, LICOR Inc., Lincoln, NE,

USA). After washing, the PVDF membranes and biomaterials were scanned on the 800 nm channel of the Odyssey CLx IR Imaging System (LICOR Inc.). The relative fluorescence of biomaterials incubated with HBSS only was subtracted from the relative fluorescence of the biomaterials from cell culture to remove background fluorescence, and the mass of IgG was interpolated from a standard curve. For the biomaterials, IgG adsorption was normalized to the mass of the 8-mm diameter sample.

2.7 Receptor Blocking

To block receptors, neutrophils were incubated with 10 μg/mL Fab blocking fragments for FcγRI (Cat. No. 216-580, Ancell, Bayport, MN, USA), FcγRIIa (Cat. No. 181-580, Ancell, Bayport, MN, USA), and FcγRIIIb (Cat. No. 165-580, Ancell, Bayport, MN, USA) and a blocking antibody for CD11b (Cat. No. BDB553308, Fisher Scientific, Waltham, MA, USA) at 37°C for 10 minutes. IgG Fab (Cat. No. 278-580, Ancell, Bayport, MN, USA) and IgG (Cat. No 401401, BioLegend, San Diego, CA, USA) were used as isotype controls. After resuspending, neutrophils were seeded on the biomaterials (n = 4) that were hydrated with 40 μL of cell culture media. Untreated cells seeded on the biomaterials (n = 4) served as controls.

2.8 Inhibition of TAK1

In order to inhibit signaling through TAK1, neutrophils were incubated with 10 nM 5Z-7-oxozeaenol (Cat. No. 49-961-01MG, Fisher Scientific, Waltham, MA, USA) or 0.1% DMSO as a negative control on ice for 30 minutes [35]. After resuspending, neutrophils were seeded on the biomaterials (n = 6) that were hydrated with 40 μL of cell culture media. Untreated cells seeded on the biomaterials (n = 4) served as controls.

2.9 Quantification of NET Release

The release of NETs was quantified by measuring the concentration of NET-dissociated MPO in the cell culture supernatant using an MPO Human Instant ELISA Kit (Cat. No. BMS2038INST, Thermo Fisher Scientific, Waltham, MA, USA) [10, 17, 43]. Briefly, the cell culture supernatants were transferred to a clean cell culture plate and centrifuged at 500 xg for 5 minutes to pellet any free neutrophils. Then, 50 μL of the centrifuged supernatant was collected and assayed using the MPO Human Instant ELISA Kit following manufacturer instructions. To quantify percent NET release on the biomaterials, the concentration of MPO was normalized to the concentration of MPO in the TCP positive control at 6 hours, representing maximum NET release.

2.10 Fluorescence Microscopy

Samples were stained with 5 μM SYTOX orange (Cat. No. S34861, Thermo Fisher Scientific, Waltham, MA, USA) and NucBlue™ Fixed Cell ReadyProbes™ Reagent (DAPI, Cat. No. R37606, Thermo Fisher Scientific, Waltham, MA, USA) and imaged as previously described [10]. Samples were incubated sequentially for 5 minutes at room temperature with each stain. Three washes with PBS for 5 minutes each were performed between each stain. The stained cells and NETs were visualized on an Olympus BX43 fluorescent microscope,

and images were acquired in cellSens Standard 1.9 (Olympus Corp.). After image acquisition, contrast was enhanced using the automated function in cellSens.

2.11 Statistical Analysis

Statistically significant differences between fiber diameters were determined using a Mann-Whitney test. Statistical differences for the depletion of IgG were determined using a Kruskal-Wallis test with Dunn's multiple comparisons procedure. All other differences were tested with an ANOVA and Holm-Sidak's multiple comparisons test. Statistical analyses were performed in Prism version 8.4.3 (GraphPad Software, San Diego, CA, USA) at a significance level of 0.05. Data are reported as mean ± standard deviation.

3. Results

3.1 Electrospun PDO Biomaterials Were Fabricated with Small and Large Fibers

PDO was electrospun to create small and large fibers (Figure 1A). The average fiber diameters for the small and large fibers are 0.4 ± 0.1 μm and 2.1 ± 0.4 μm, respectively (Figure 1B). The small fiber biomaterials up-regulate the release of NETs while absorbing 2-times more IgG on their surface compared to large fibers when normalized to the biomaterial mass, suggesting a role for increased IgG signaling in biomaterial-induced NET release [7, 31]. As in our prior work, these small and large fiber electrospun biomaterials allow us to further probe the role of IgG in biomaterial-induced NET release.

3.2 IgG Increases NET Release

Neutrophils were isolated from the whole blood of healthy donors and seeded on electrospun biomaterials with increasing masses of IgG in the absence of other surface-adsorbed proteins to examine the potential stimulatory role of IgG in biomaterial-induced NET release (Figure 2A). As expected, the addition of IgG resulted in an increased adsorption of IgG to the biomaterial surfaces prior to seeding the neutrophils (Figure 2B). For the control biomaterials, the neutrophils had an increased propensity to release NETs on the small fibers compared to the large fibers (Figure 2C) with nearly 2-times the release of NETs on small fibers. With the addition of 1 μg of IgG, the release of NETs was similar to the level of the controls on both small and large fibers. With the addition of 100 μg of IgG to saturate the surface of the biomaterials, NET release was significantly increased on both the small and large fiber biomaterials. Moreover, the release of NETs on the large fibers was increased to the level of the small fibers, indicating a stimulatory effect for IgG independent of fiber size when experimentally increased. The trends were similar with the addition of 440 μg of IgG, or IgG at physiological concentration, but there was no further increase in NET release observed. Together, these dose-response data indicate that IgG stimulates biomaterial-induced NET release when artificially increased in the absence of other surface-adsorbed proteins.

3.3. Depleting IgG Decreases Adsorption and Modulates NET Release

In addition to stimulating NET release with the addition of IgG, we also examined if the depletion of IgG from autologous serum would modulate NET release. First, we developed a method to deplete IgG using Dynabeads™ protein G (Figure 3A). For both an isotype

control of IgG and the autologous serum, our depletion protocol resulted in greater than 97% reduction in IgG concentration. For the isotype control, the concentration dropped from 11.1 ± 4.0 mg/mL to 0.30 ± 0.03 mg/mL. For the autologous serum, the concentration was reduced from 10.9 ± 2.8 mg/mL to 0.08 ± 0.05 mg/mL. To verify that this reduction translated to a reduction in biomaterial surface-adsorbed IgG, we quantified IgG adsorption on the small and large fibers both prior to seeding the neutrophils (Figure 3B) and after culture with neutrophils (Figure 3C). As expected, nearly 2-times the mass of IgG was adsorbed on the small electrospun fibers compared to the large fibers when the biomaterials were hydrated with cell culture media containing 0.2% autologous serum. However, when the biomaterials were hydrated with the IgG-depleted serum, the adsorption of IgG was significantly reduced on both small and large fibers to 0.4 ± 0.3 ng and 0.9 ± 0.6 ng, respectively, verifying that the depletion of IgG from the cell culture media translates to reduced surface adsorption. Interestingly, although surface-adsorbed IgG was reduced by nearly 95% on both biomaterials prior to cell seeding, the reduction in surface-adsorbed IgG was less apparent after culturing the neutrophils for 3 hours (Figure 3C) due to the addition of IgG within the cell culture media and the dynamic nature of protein adsorption on our biomaterials [31]. We then quantified the release of NETs in response to the modulated IgG adsorption (Figure 3D) and found that the release of NETs trended towards a decrease on the small fibers ($p < 0.1$), but did not change on the large fibers (Figure 3E). These data suggest that decreasing surface-adsorbed IgG modulates NET release, but the data are not significant because of the rapid adsorption of IgG from autologous serum.

3.4 Blocking FcγIIIb Decreases Biomaterial-Induced NET Release

Next, we blocked FcγRI, FcγRIIa, FcγRIIIb, and CD11b to test their potential contribution to NET release. On the small fiber biomaterials (Figure 4A and C), blocking of FcγRIIIb led to a significant reduction in NET release to approximately half of the control, similar to the findings of others [34, 35], whereas blocking of FcγRI, FcγRIIa, and CD11b resulted in no change in NET release. Contrastingly, NET release was near equivalent on the large fiber biomaterials with no change in NET release upon blocking any of the receptors (Figure 4B and D). Given that blocking of FcγRIIIb on the small fiber biomaterials reduced NET release to the level of the large fiber biomaterials, the data suggest that ligation of FcγRIIIb and its subsequent signaling are involved in biomaterial-induced NET release.

3.5 Inhibition of FcγRIIIb Signaling through TAK1 Attenuates NET Release

To further verify the involvement of FcγIIIb in biomaterial-induced NET release, we inhibited TAK1, an enzyme required for FcγIIIb signaling in NET release [35]. Inhibition of TAK1 with the selective inhibitor 5Z-7-oxozeaenol led to a significant reduction in NET release on both the small and large fiber biomaterials (Figure 5A and B). On the small fibers, NET release decreased from 13.5 ± 4.7% to 4.3 ± 2.7%, a two-fold decrease. On the large fibers, the release of NETs was reduced from 7.2 ± 2.0% to 3.3 ± 0.6%, which is roughly the same level of NET release as the TCP control. Taken together, these data indicate ligation of FcγIIIb with IgG and subsequent signaling through TAK1 participate in electrospun biomaterial-induced NET release.

4. Discussion

Electrospun biomaterials offer putative advantages for *in situ* tissue engineering applications because of their versatile biomimetic structure, relatively simple fabrication, and cost-effectiveness. However, understanding the inflammatory and immune response to these biomaterials for guided tissue regeneration is a challenge that requires further investigation for translation into the clinical environment. Recently, our group and others have investigated the activation of neutrophils and release of NETs in response to biomaterials [7, 26, 27, 44]. The dysregulated release of NETs contributes to inflammation and fibrosis in several pathologies due to the release of toxic cargo and the localization of inflammatory adjuvants, like tissue factor, and has been described for thrombosis, cancer, and biomaterials *in vivo*, including our electrospun biomaterials [7, 20–26, 44–45]. In addition, multiple inflammatory diseases are linked to IC-induced NET release, including systemic lupus erythematosus [46], rheumatoid arthritis [47], anaphylaxis [48], and small vessel vasculitis [49]. Previously, we showed that greater IgG adsorption occurs on high surface area biomaterials that up-regulate NET release [31], but it remained unclear whether this surface-adsorbed IgG is responsible for stimulating biomaterial-induced NET formation similar to IC-induced NET release. Here, we demonstrate for the first time that IgG adsorption, binding to FcγRIIIb, and signaling through TAK1 stimulates and regulates the *in vitro* release of NETs from human neutrophils on the surface of electrospun PDO biomaterials.

The binding of neutrophils to ICs and biomaterials is an important mechanism for innate immunity, the activation of neutrophils, and inflammation. IC-induced NET release requires opsonization of the antigen or pathogen with IgG to mediate FcγR binding and has been shown to occur *in vitro* in the context of soluble and immobilized ICs and IgG-coated beads [33, 34, 50]. In this work, we found that increasing the surface-adsorbed IgG in the absence of other proteins on our biomaterials up-regulated the release of NETs, which occurred independent of electrospun fiber size. When the concentration of IgG exceeded the mass needed to saturate the material surface, no further increase in NET release was observed, indicating that the IgG must be bound to the material surface to have a stimulatory effect. Indeed, the high concentration of IgG in circulation does not stimulate NET release from circulating neutrophils, and others have shown that free Fc fragments not bound to a substrate and free IgG were unable to stimulate NET formation in the context of ICs [51, 52]. Likewise, we also showed that a transient decrease in surface-adsorbed IgG down-regulated the release of NETs, but this occurred in a fiber size dependent manner and the results were not significant due to the small sample size and biological variability (see Supplementary Spreadsheet 1). Transient reduction of IgG adsorption on the small fibers, but not the large fibers, trended towards a reduction in NET release, suggesting that other adsorbed proteins may also participate in stimulating or regulating NET release on our biomaterials [28, 31]. Nonetheless, given the magnitude of IgG adsorption on the biomaterial surface, our data provide evidence for IgG as a stimulatory and regulatory protein in electrospun biomaterial-induced NET release.

Several FcγRs can bind IgG and induce outside-in signaling to trigger the release of NETs. Both FcγRIIa and FcγRIIIb have been implicated in IC-induced NET release through their independent engagement and cooperative signaling [33, 34, 37]. Additionally, Mac-1 has

been found to participate in FcγRIIIb-induced NET formation both through its activation and crosstalk with other receptors through shared signaling molecules [34]. Although it is not constitutively expressed, FcγRI is up-regulated within several hours of neutrophil activation, indicating it may also bind IgG during an inflammatory response [38–40]. In our experiments, we found that blocking of FcγRIIIb significantly attenuated NET release on the small fiber biomaterials to the level of the large fibers whereas blocking of FcγRI, FcγRIIa, or CD11b had no significant effect. Despite the decrease observed on the small fiber biomaterials, we found that blocking of FcγRIIIb had no effect on the large fiber biomaterials, suggesting potential confirmation or valency differences, or the presence of another stimulus and compensatory mechanism of NET release when FcγRIIIb is blocked [28, 33]. Multiple stimuli or a compensatory mechanism may also explain why NET release was reduced but not completely abrogated on the small fiber biomaterials upon blocking FcγRIIIb. Moreover, the release of NETs is an active process that occurs after direct neutrophil contact with the stimulus, and others have demonstrated the ability of the neutrophil to modulate its response based on the stimuli, their size, and their valency [16, 33].

FcγRIIIb is a glycosylphosphatidylinositol (GPI)-linked receptor that lacks transmembrane and cytoplasmic domains [53]. Compared to FcγRIIa, FcγRIIIb is 4- to 5-fold more abundant on the neutrophil membrane and is highly mobile with the ability to protrude further due to its GPI anchor [54, 55]. Despite lacking a transmembrane and cytoplasmic domain, FcγRIIIb signaling for NET release occurs through TAK1 and is dependent on NADPH oxidase (NOX) and ERK activation [34, 35, 56]. To further demonstrate the involvement of FcγRIIIb in biomaterial-induced NET release, we blocked TAK1 and showed a significant decrease in NETs on both small and large fiber biomaterials. The decrease in NET release on both biomaterials was unexpected because we did not observe a decrease in NETs on the large fibers when surface adsorbed IgG was reduced. However, TAK1 can be activated by other receptors, including Toll like receptors, indicating that multiple signaling pathways may participate in biomaterial-induced NET release [28, 57]. When NOX is activated downstream of TAK1, reactive oxygen species are produced, which can in turn activate peptidyl arginine deiminase 4 (PAD4) to citrullinate histones and enhance NET generation [58]. We previously showed that citrullinated histones are found in biomaterial-induced NETs and that we could inhibit biomaterial-induced NET release using Cl-amidine, an inhibitor of PAD4, but were unable to explain the pathway leading to PAD4 activation [7, 8]. Given that ligation of FcγRIIa has been found to activate PAD4 [37], our present study suggests that for our electrospun biomaterials, PAD4 activation is linked to IgG engagement of FcγRIIIb and signaling through TAK1, although the precise mechanism remains to be explored.

The adsorption of IgG to the surface of biomaterials has long been considered significant in the design of biocompatible biomaterials that regulate inflammation, and IgG adsorption is consistently observed on many different biomaterial surfaces [59–63]. Prior work has focused on the adsorption of IgG as an activator of complement and monocytes [59, 63], but one group has explored IgG adsorption on expanded polytetrafluoroethylene and its impact on neutrophil activation and phagocytosis for preventing infection [60, 61]. To our knowledge, we are the first to explore the role of IgG adsorption in biomaterial-induced

NET release in tissue engineering applications. Because we now know that neutrophils are important effector cells in the response to biomaterials [6], our work highlights the importance of considering IgG adsorption in the context of preconditioning biomaterial-neutrophil interactions that could nucleate fibrosis, thrombosis, or chronic inflammation. Future investigations are needed to determine if protein adsorption can be regulated independent of fiber size and how altering the protein adsorption profile impacts NET release and subsequent inflammation, thrombosis, fibrosis, and the potential for tissue healing *in vivo*. Ultimately, we have demonstrated that surface adsorbed IgG, ligation of FcγRIIIb, and activation of TAK1 are involved in electrospun biomaterial-induced NET release, and modulation of this pathway may have beneficial therapeutic effects for regulating neutrophil-mediated inflammation, fibrosis, and *in situ* tissue regeneration.

5. Conclusion

Electrospun biomaterials have great potential for a variety of *in situ* tissue engineering applications, but regulating the neutrophil-driven inflammatory response to promote tissue regeneration remains a challenge. In our prior work, we found that IgG adsorption on electrospun PDO is 100- to 200-times greater than the adsorption of other serum proteins and that it may be linked to the increased propensity to form NETs on electrospun biomaterials. The results presented here demonstrate that *in vitro* IgG adsorption does in fact stimulate and regulate biomaterial-induced NET release through FcγRIIIb and activation of TAK1. While the present study only investigated electrospun PDO with differing fiber sizes in the context of tissue engineering, these data garner important insights that are applicable to the design of other biomaterials, including degradable and non-degradable devices. More broadly, an understanding of how adsorbed proteins regulate NET formation during the acute inflammatory response can facilitate the design of new biomaterials for the desired biological outcome, set in motion by the neutrophil and its effector functions.

Supplementary Material

Refer to Web version on PubMed Central for supplementary material.

Funding:

This work was supported by the National Institutes of Health [R15EB022345] and the National Science Foundation Graduate Research Fellowship Program [1451514].

References

[1]. Lannutti J, Reneker D, Ma T, Tomasko D, Farson D, Electrospinning for tissue engineering scaffolds, J. Mater. Chem 27(3) (2007) 504–509.

[2]. Kelleher CM, Vacanti JP, Engineering extracellular matrix through nanotechnology, J. R. Soc. Interface 7 (2010) S717–S729. [PubMed: 20861039]

[3]. Afonso PV, Janka-Junttila M, Lee YJ, McCann CP, Oliver CM, Aamer KA, Losert W, Cicerone MT, Parent CA, LTB4 is a signal-relay molecule during neutrophil chemotaxis, Dev. Cell 22(5) (2012) 1079–1091. [PubMed: 22542839]

[4]. Li Q, Ma L, Gao C, Biomaterials for in situ tissue regeneration: development and perspectives, J. Mater. Chem 3(46) (2015) 8921–8938.

[5]. Anderson JM, Biological responses to materials, Annu. Rev. Mater. Res 31(1) (2001) 81–110.

[6]. Selders GS, Fetz AE, Radic MZ, Bowlin GL, An overview of the role of neutrophils in innate immunity, inflammation and host-biomaterial integration, Regen. Biomat 4(1) (2017) 55–68.

[7]. Fetz AE, Neeli I, Rodriguez IA, Radic MZ, Bowlin GL, Electrospun template architecture and composition regulate neutrophil NETosis in vitro and in vivo, Tissue Engin. Part A (2017).

[8]. Fetz AE, Neeli I, Buddington KK, Read RW, Smeltzer MP, Radic MZ, Bowlin GL, Localized delivery of Cl-amidine from electrospun polydioxanone templates to regulate acute neutrophil NETosis: A preliminary evaluation of the PAD4 inhibitor for tissue engineering, Front. Pharmacol 9 (2018) 289. [PubMed: 29643810]

[9]. Minden-Birkenmaier BA, Cherukuri K, Smith RA, Radic MZ, Bowlin GL, Manuka honey modulates the inflammatory behavior of a dHL-60 neutrophil model under the cytotoxic limit, Int. J. Biomater 2019 (2019).

[10]. Minden-Birkenmaier BA, Smith RA, Radic MZ, van der Merwe M, Bowlin GL, Manuka honey reduces NETosis on an electrospun template within a therapeutic window, Polymers 12(6) (2020) 1430.

[11]. Minden-Birkenmaier BA, Meadows MB, Cherukuri K, Smeltzer MP, Smith RA, Radic MZ, Bowlin GL, The effect of manuka honey on dHL-60 cytokine, chemokine, and matrix-degrading enzyme release under inflammatory conditions, Med one 4(2) (2019).

[12]. Anderson JM, Rodriguez A, Chang DT, Foreign body reaction to biomaterials, Semin. Immunol, Elsevier, 2008, pp. 86–100.

[13]. Piccard H, Muschel RJ, Opdenakker G, On the dual roles and polarized phenotypes of neutrophils in tumor development and progression, Crit. Rev. Oncol. Hematol 82(3) (2012) 296–309. [PubMed: 21798756]

[14]. Fridlender ZG, Sun J, Kim S, Kapoor V, Cheng G, Ling L, Worthen GS, Albelda SM, Polarization of tumor-associated neutrophil phenotype by TGF-β:“N1” versus “N2” TAN, Cancer Cell 16(3) (2009) 183–194. [PubMed: 19732719]

[15]. Brinkmann V, Reichard U, Goosmann C, Fauler B, Uhlemann Y, Weiss DS, Weinrauch Y, Zychlinsky A, Neutrophil extracellular traps kill bacteria, Science 303(5663) (2004) 1532–1535. [PubMed: 15001782]

[16]. Branzk N, Lubojemska A, Hardison SE, Wang Q, Gutierrez MG, Brown GD, Papayannopoulos V, Neutrophils sense microbe size and selectively release neutrophil extracellular traps in response to large pathogens, Nat. Immunol 15(11) (2014) 1017–25. [PubMed: 25217981]

[17]. Parker H, Albrett AM, Kettle AJ, Winterbourn CC, Myeloperoxidase associated with neutrophil extracellular traps is active and mediates bacterial killing in the presence of hydrogen peroxide, J. Leuko. Biol 91(3) (2012) 369–376. [PubMed: 22131345]

[18]. Kaplan MJ, Radic M, Neutrophil extracellular traps: Double-edged swords of innate immunity, J. Immunol 189(6) (2012) 2689–2695. [PubMed: 22956760]

[19]. Wong SL, Demers M, Martinod K, Gallant M, Wang Y, Goldfine AB, Kahn CR, Wagner DD, Diabetes primes neutrophils to undergo NETosis, which impairs wound healing, Nat. Med 21(7) (2015) 815–9. [PubMed: 26076037]

[20]. Radic M, Marion TN, Neutrophil Extracellular Chromatin Traps Connect Innate Immune Response to Autoimmunity, Semin. Immunopathol 35(4) (2013) 465–80. [PubMed: 23595413]

[21]. Demers M, Krause DS, Schatzberg D, Martinod K, Voorhees JR, Fuchs TA, Scadden DT, Wagner DD, Cancers predispose neutrophils to release extracellular DNA traps that contribute to cancer-associated thrombosis, Proc. Natl. Acad. Sci. U. S. A 109(32) (2012) 13076–13081. [PubMed: 22826226]

[22]. Albrengues J, Shields MA, Ng D, Park CG, Ambrico A, Poindexter ME, Upadhyay P, Uyeminami DL, Pommier A, Küttner V, Neutrophil extracellular traps produced during inflammation awaken dormant cancer cells in mice, Science 361(6409) (2018).

[23]. Chrysanthopoulou A, Mitroulis I, Apostolidou E, Arelaki S, Mikroulis D, Konstantinidis T, Sivridis E, Koffa M, Giatromanolaki A, Boumpas DT, Neutrophil extracellular traps promote differentiation and function of fibroblasts, J. Pathol 233(3) (2014) 294–307. [PubMed: 24740698]

[24]. Martinod K, Demers M, Fuchs TA, Wong SL, Brill A, Gallant M, Hu J, Wang Y, Wagner DD, Neutrophil histone modification by peptidylarginine deiminase 4 is critical for deep vein

thrombosis in mice, Proc. Natl. Acad. Sci. U. S. A 110(21) (2013) 8674–8679. [PubMed: 23650392]

[25]. Riehl DR, Roewe J, Klebow S, Esmon NL, Eming S, Colucci G, Schäfer K, Gunzer M, Waisman A, Ward PA, Neutrophil extracellular traps drive bleomycin-induced lung fibrosis by regulating TGFβ1-dependent interactions of platelets and macrophages, FASEB J 30(1 Supplement) (2016) 50.1–50.1.

[26]. Jhunjhunwala S, Aresta-DaSilva S, Tang K, Alvarez D, Webber MJ, Tang BC, Lavin DM, Veiseh O, Doloff JC, Bose S, Neutrophil responses to sterile implant materials, PLoS One 10(9) (2015) e0137550.

[27]. Abaricia JO, Shah AH, Musselman RM, Olivares-Navarrete R, Hydrophilic titanium surfaces reduce neutrophil inflammatory response and NETosis, Biomaterials Science 8(8) (2020) 2289–2299. [PubMed: 32163073]

[28]. Kenny EF, Herzig A, Krüger R, Muth A, Mondal S, Thompson PR, Brinkmann V, Von Bernuth H, Zychlinsky A, Diverse stimuli engage different neutrophil extracellular trap pathways, Immunol. Cell Biol 6 (2017) e24437.

[29]. Hoppenbrouwers T, Autar AS, Sultan AR, Abraham TE, van Cappellen WA, Houtsmuller AB, van Wamel WJ, van Beusekom HM, van Neck JW, de Maat MP, In vitro induction of NETosis: Comprehensive live imaging comparison and systematic review, PLoS One 12(5) (2017) e0176472.

[30]. Gray RD, Lucas CD, MacKellar A, Li F, Hiersemenzel K, Haslett C, Davidson DJ, Rossi AG, Activation of conventional protein kinase C (PKC) is critical in the generation of human neutrophil extracellular traps, Journal of Inflammation 10(1) (2013) 12. [PubMed: 23514610]

[31]. Fetz AE, Fantaziu CA, Smith RA, Radic MZ, Bowlin GL, Surface area to volume ratio of electrospun polydioxanone templates regulates the adsorption of soluble proteins from human serum, Bioeng. 6(3) (2019) 78.

[32]. Unkeless JC, Shen Z, Lin C-W, DeBeus E, Function of human FcγRIIA and FcγRIIIB, Semin. Immunol, Elsevier, 1995, pp. 37–44.

[33]. Chen K, Nishi H, Travers R, Tsuboi N, Martinod K, Wagner DD, Stan R, Croce K, Mayadas TN, Endocytosis of soluble immune complexes leads to their clearance by FcγRIIIB but induces neutrophil extracellular traps via FcγRIIA in vivo, Blood (2012) 4421–4431. [PubMed: 22955924]

[34]. Behnen M, Leschczyk C, Möller S, Batel T, Klinger M, Solbach W, Laskay T, Immobilized immune complexes induce neutrophil extracellular trap release by human neutrophil granulocytes via FcγRIIIB and Mac-1, J. Immunol (2014) 1400478.

[35]. Alemán OR, Mora N, Cortes-Vieyra R, Uribe-Querol E, Rosales C, Transforming growth factor-β-activated kinase 1 is required for human FcγRIIIb-induced neutrophil extracellular trap formation, Front. Immunol 7 (2016) 277. [PubMed: 27486461]

[36]. Short KR, von Köckritz-Blickwede M, Langereis JD, Chew KY, Job ER, Armitage CW, Hatcher B, Fujihashi K, Reading PC, Hermans PW, Antibodies mediate formation of neutrophil extracellular traps in the middle ear and facilitate secondary pneumococcal otitis media, J. Infect 82(1) (2014) 364–370.

[37]. Perdomo J, Leung HH, Ahmadi Z, Yan F, Chong JJ, Passam FH, Chong BH, Neutrophil activation and NETosis are the major drivers of thrombosis in heparin-induced thrombocytopenia, Nature 10(1) (2019) 1–14.

[38]. Guyre PM, Campbell AS, Kniffin WD, Fanger MW, Monocytes and polymorphonuclear neutrophils of patients with streptococcal pharyngitis express increased numbers of type I IgG Fc receptors, J. Clin. Invest 86(6) (1990) 1892–1896. [PubMed: 2147695]

[39]. Repp R, Valerius T, Sendler A, Gramatzki M, Iro H, Kalden J, Platzer E, Neutrophils express the high affinity receptor for IgG (Fc gamma RI, CD64) after in vivo application of recombinant human granulocyte colony-stimulating factor, Blood (1991).

[40]. Davis BH, Improved diagnostic approaches to infection/sepsis detection, Expert Rev. Mol. Diagn 5(2) (2005) 193–207. [PubMed: 15833049]

[41]. Neeli I, Radic M, Opposition between PKC isoforms regulates histone deimination and neutrophil extracellular chromatin release, Front. Immunol 4 (2013) 38. [PubMed: 23430963]

[42]. Kudva IT, Griffin RW, Garren JM, Calderwood SB, John M, Identification of a protein subset of the anthrax spore immunome in humans immunized with the anthrax vaccine adsorbed preparation, Infect. Immun 73(9) (2005) 5685–5696. [PubMed: 16113286]

[43]. Fetz AE, King WE, Minden-Birkenmaier BA, Bowlin GL, Methods for quantifying neutrophil extracellular traps on biomaterials, Bioeng. Tech, Humana, In Press.

[44]. Won JE, Lee YS, Park JH, Lee JH, Shin YS, Kim CH, Knowles JC, Kim HW, Hierarchical microchanneled scaffolds modulate multiple tissue-regenerative processes of immune-responses, angiogenesis, and stem cell homing, Biomaterials 227 (2020) 119548. [PubMed: 31670033]

[45]. Kambas J K, Chrysanthopoulou A, Vassilopoulos D, Apostolidou E, Skendros P, Girod A, Arelaki S, Froudarakis M, Nakopoulou L, Giatromanolaki A, Tissue factor expression in neutrophil extracellular traps and neutrophil derived microparticles in antineutrophil cytoplasmic antibody associated vasculitis may promote thromboinflammation and the thrombophilic state associated with the disease, Ann. Rheum. Dis 73(10) (2014) 1854–63. [PubMed: 23873874]

[46]. Van Der Linden M, Westerlaken GH, Van Der Vlist M, Van Montfrans J, Meyaard L, Differential signalling and kinetics of neutrophil extracellular trap release revealed by quantitative live imaging, Sci. Rep 7(1) (2017) 1–11. [PubMed: 28127051]

[47]. Aleyd E, Al M, Tuk CW, van der Laken CJ, van Egmond M, IgA complexes in plasma and synovial fluid of patients with rheumatoid arthritis induce neutrophil extracellular traps via FcαRI, J. Immunol 197(12) (2016) 4552–4559. [PubMed: 27913645]

[48]. Jönsson F, Mancardi DA, Kita Y, Karasuyama H, Iannascoli B, Van Rooijen N, Shimizu T, Daëron M, Bruhns P, Mouse and human neutrophils induce anaphylaxis, J. Clin. Invest 121(4) (2011) 1484–1496. [PubMed: 21436586]

[49]. Bergqvist C, Safi R, El Hasbani G, Abbas O, Kibbi A, Nassar D, Neutrophil Extracellular Traps are Present in Immune-complex-mediated Cutaneous Small Vessel Vasculitis and Correlate with the Production of Reactive Oxygen Species and the Severity of Vessel Damage, Acta Derm. Venereol (2019).

[50]. Saffarzadeh M, Cabrera-Fuentes HA, Veit F, Jiang D, Scharffetter-Kochanek K, Gille C, Rooijakkers SH, Hartl D, Preissner KTJD, Characterization of rapid neutrophil extracellular trap formation and its cooperation with phagocytosis in human neutrophils, 2(2) (2014) e19.

[51]. Kraaij T, Tengström FC, Kamerling SW, Pusey CD, Scherer HU, Toes RE, Rabelink TJ, van Kooten C, Teng YO, A novel method for high-throughput detection and quantification of neutrophil extracellular traps reveals ROS-independent NET release with immune complexes, Autoimmun. Rev 15(6) (2016) 577–584. [PubMed: 26925759]

[52]. Nimmerjahn F, Ravetch JV, Fcγ receptors as regulators of immune responses, Nat. Rev. Immunol 8(1) (2008) 34–47. [PubMed: 18064051]

[53]. Tosi M, Berger M, Functional differences between the 40 kDa and 50 to 70 kDa IgG Fc receptors on human neutrophils revealed by elastase treatment and antireceptor antibodies, J. Immunol 141(6) (1988) 2097–2103. [PubMed: 2844894]

[54]. Selvaraj P, Rosse WF, Silber R, Springer TA, The major Fc receptor in blood has a phosphatidylinositol anchor and is deficient in paroxysmal nocturnal haemoglobinuria, Nature 333(6173) (1988) 565–567. [PubMed: 2967435]

[55]. Alemán OR, Mora N, Cortes-Vieyra R, Uribe-Querol E, Rosales C, Differential use of human neutrophil Fcγ receptors for inducing neutrophil extracellular trap formation, J. Immnol. Res 2016 (2016).

[56]. Yu L, Wang L, Chen S, Endogenous toll-like receptor ligands and their biological significance, J. Cell Molec. Med 14(11) (2010) 2592–2603. [PubMed: 20629986]

[57]. Leshner M, Wang S, Lewis C, Zheng H, Chen XA, Santy L, Wang Y, PAD4 mediated histone hypercitrullination induces heterochromatin decondensation and chromatin unfolding to form neutrophil extracellular trap-like structures, Front. Immunol 3 (2012) 307. [PubMed: 23060885]

[58]. Battiston K, Ouyang B, Honarparvar E, Qian J, Labow R, Simmons C, Santerre J, Interaction of a block-co-polymeric biomaterial with immunoglobulin G modulates human monocytes towards a non-inflammatory phenotype, Acta Biomater. 24 (2015) 35–43. [PubMed: 26074158]

[59]. De La Cruz C, Haimovich B, Greco RS, Immobilized IgG and fibrinogen differentially affect the cytoskeletal organization and bactericidal function of adherent neutrophils, J. Surg. Res 80(1) (1998) 28–34. [PubMed: 9790811]

[60]. Katz DA, Haimovich B, Greco RS, FcγRII, FcγRIII, and CD18 receptors mediate in part neutrophil activation on a plasma coated expanded polytetrafluoroethylene surface, Surgery 118(2) (1995) 154–161. [PubMed: 7638728]

[61]. Hulander M, Lundgren A, Berglin M, Ohrlander M, Lausmaa J, Elwing H, Immune complement activation is attenuated by surface nanotopography, Int. J. Nanomedicine 6 (2011) 2653. [PubMed: 22114496]

[62]. Hiraishi K, Takeda Y, Shiobara N, Shibusawa H, Jimma F, Kashiwagi N, Saniabadi AR, Adachi M, Studies on the mechanisms of leukocyte adhesion to cellulose acetate beads: an in vitro model to assess the efficacy of cellulose acetate carrier-based granulocyte and monocyte adsorptive apheresis, Ther. Apher. Dial 7(3) (2003) 334–340. [PubMed: 12924609]

[63]. Nilsson B, Ekdahl KN, Mollnes TE, Lambris JD, The role of complement in biomaterial-induced inflammation, Mol. Immunol 44(1–3) (2007) 82–94. [PubMed: 16905192]

Statement of Significance:

Electrospun biomaterials have great potential for *in situ* tissue engineering because of their versatility and biomimetic properties. However, understanding how to design the biomaterial to regulate acute inflammation, dominated by neutrophils, remains a great challenge for successful tissue integration and regeneration. In this work, we demonstrate for the first time how protein adsorption on the biomaterial surface and engagement of a specific neutrophil receptor induces intracellular signals that regulate the pro-inflammatory release of neutrophil extracellular traps (NETs). Given the deleterious effects of NETs during the acute inflammatory response to a biomaterial, our work highlights the importance of considering biomaterial-neutrophil interactions on degradable and non-degradable biomaterials to achieve the desired biological outcome.

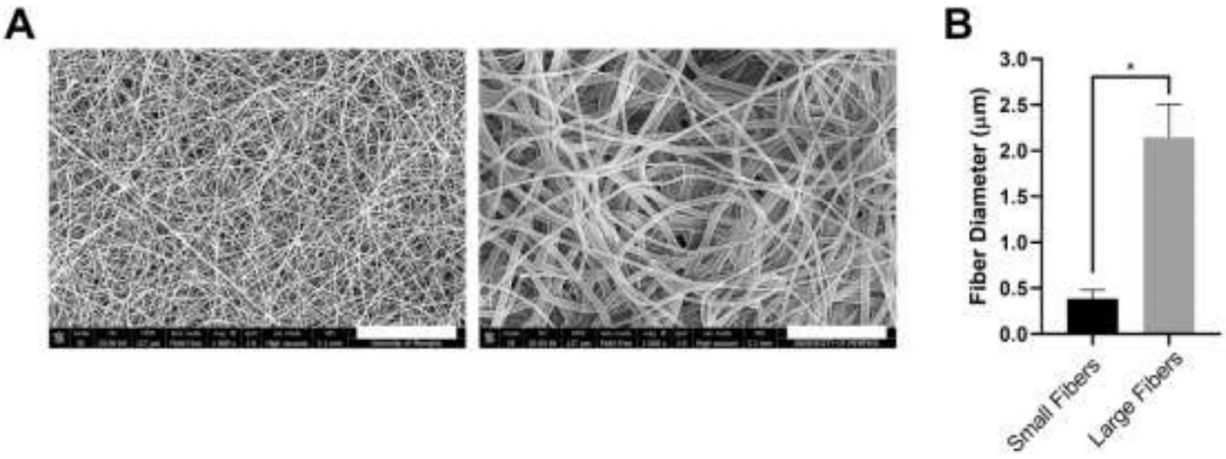

Figure 1.

Electrospun PDO biomaterials were fabricated with small and large fibers. (A) Representative SEMs of the small and large fiber biomaterials. Micrographs were acquired at 1000x magnification and scale bars are 30 μm. (B) Fiber diameters of the electrospun biomaterials. Measurements (n = 150) were taken in FibraQuant 1.3 software. * $p < 0.0001$ was determined using a Mann-Whitney test. Raw data are available in Supplementary Spreadsheet 1.

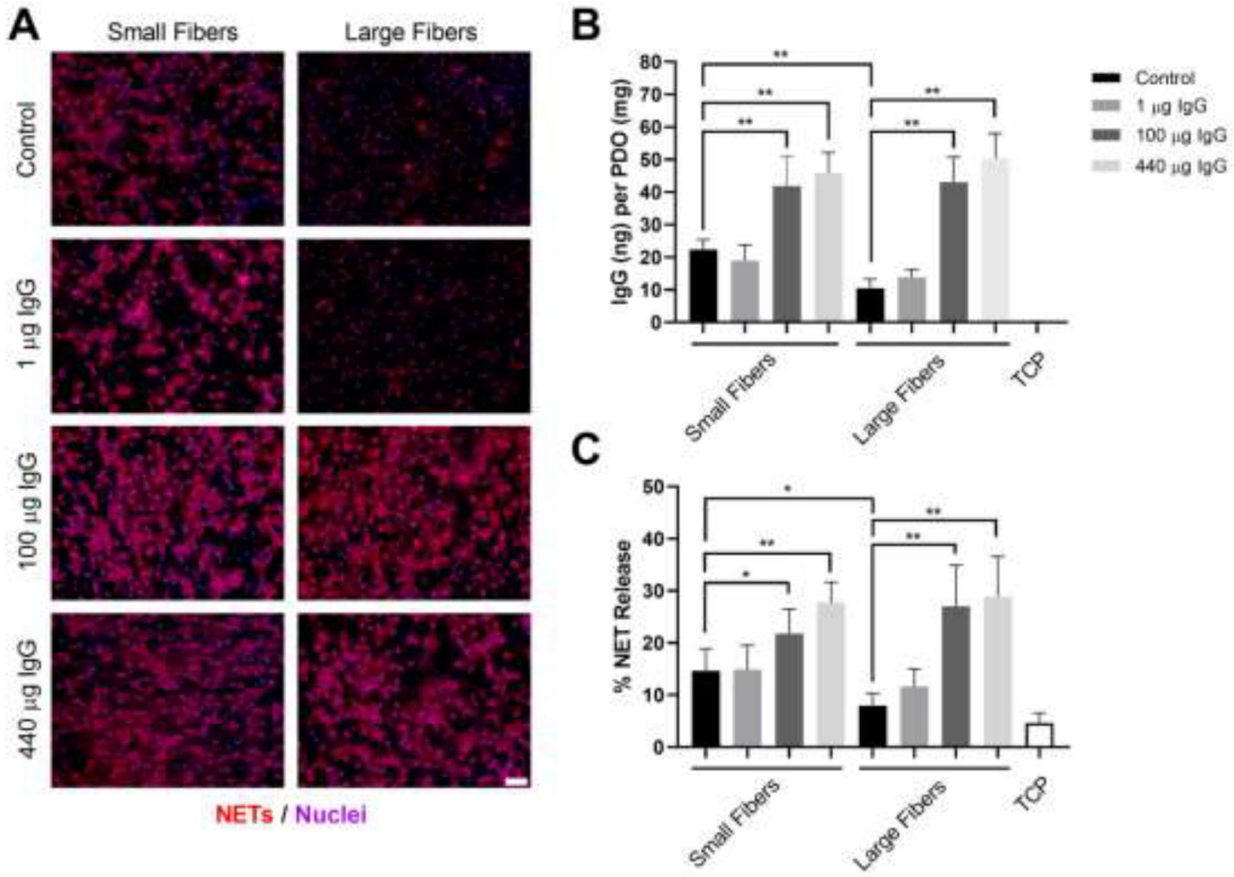

Figure 2.

Increasing IgG on the electrospun biomaterials increases NET release. (A) Fluorescent micrographs of neutrophils on the electrospun biomaterials at 3 hours after seeding. Staining of NETs (red) and nuclei (purple) reveals that increasing IgG up-regulates NET release independent of electrospun fiber size. Scale bar is 50 μm. (B) IgG adsorption on the electrospun biomaterials prior to seeding the neutrophils. (C) Percent NET release at 3 hours as quantified by the ELISA for NET-disassociated MPO. The quantification of percent NET release (n = 4) indicates that increasing IgG on the biomaterials stimulates NET release with a maximum stimulatory effect upon saturation of the material surface with 100 μg of IgG. The data represent the mean ± standard deviation of three independent experiments with unique donors. * $p < 0.05$ and ** $p < 0.0001$ were determined using an ANOVA and Holm-Sidak's multiple comparisons test. Raw data are available in Supplementary Spreadsheet 1.

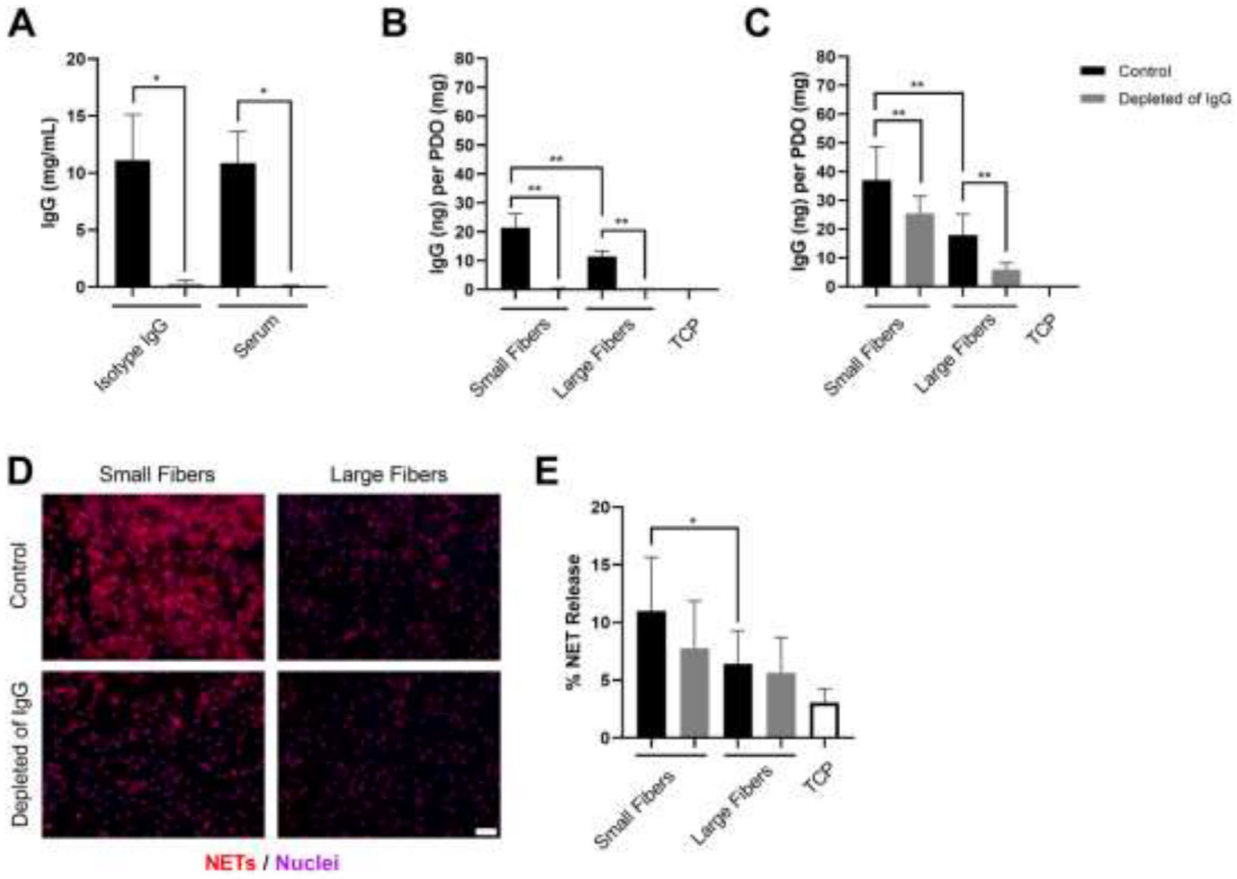

Figure 3.

Decreased IgG adsorption decreases NET release on the small but not large fiber electrospun biomaterials. (A) Concentration of IgG in isotype control (n = 3) and serum (n = 3) before and after depletion with Dynabeads™ protein G. The depletion procedure reduced the concentration of IgG by 97.4% and 99.3% for the isotype control and serum, respectively. The stock concentration of the isotype control was 11 mg/mL. * $p < 0.05$ was determined using a Kruskal-Wallis test with Dunn's multiple comparisons procedure. (B) IgG adsorption on the electrospun biomaterials prior to seeding the neutrophils. (C) IgG adsorption on the electrospun biomaterials after 3-hour culture with neutrophils. The controls hydrated with cell culture media (n = 4) adsorbed significantly more IgG compared to the samples hydrated with IgG-depleted cell culture media (n = 4) both prior to neutrophil seeding and after 3-hour culture. ** $p < 0.0001$ was determined using an ANOVA and Holm-Sidak's multiple comparisons test. (C) Fluorescent micrographs of neutrophils on the electrospun biomaterials at 3 hours after seeding. Staining of NETs (red) and nuclei (purple) reveals that decreasing IgG down-regulates NET release on small fibers. Scale bar is 50 μm. (D) Percent NET release at 3 hours as quantified by the ELISA for NET-disassociated MPO. The quantification of percent NET release (n = 4) indicates that decreasing IgG on the small fiber biomaterials decreases NET release. * $p < 0.05$ was determined using an ANOVA and Holm-Sidak's multiple comparisons test. For all graphs, the data represent the mean ± standard deviation of three independent experiments with unique donors. Individual donor

data are shown in Supplementary Figure 1. Raw data are available in Supplementary Spreadsheet 1.

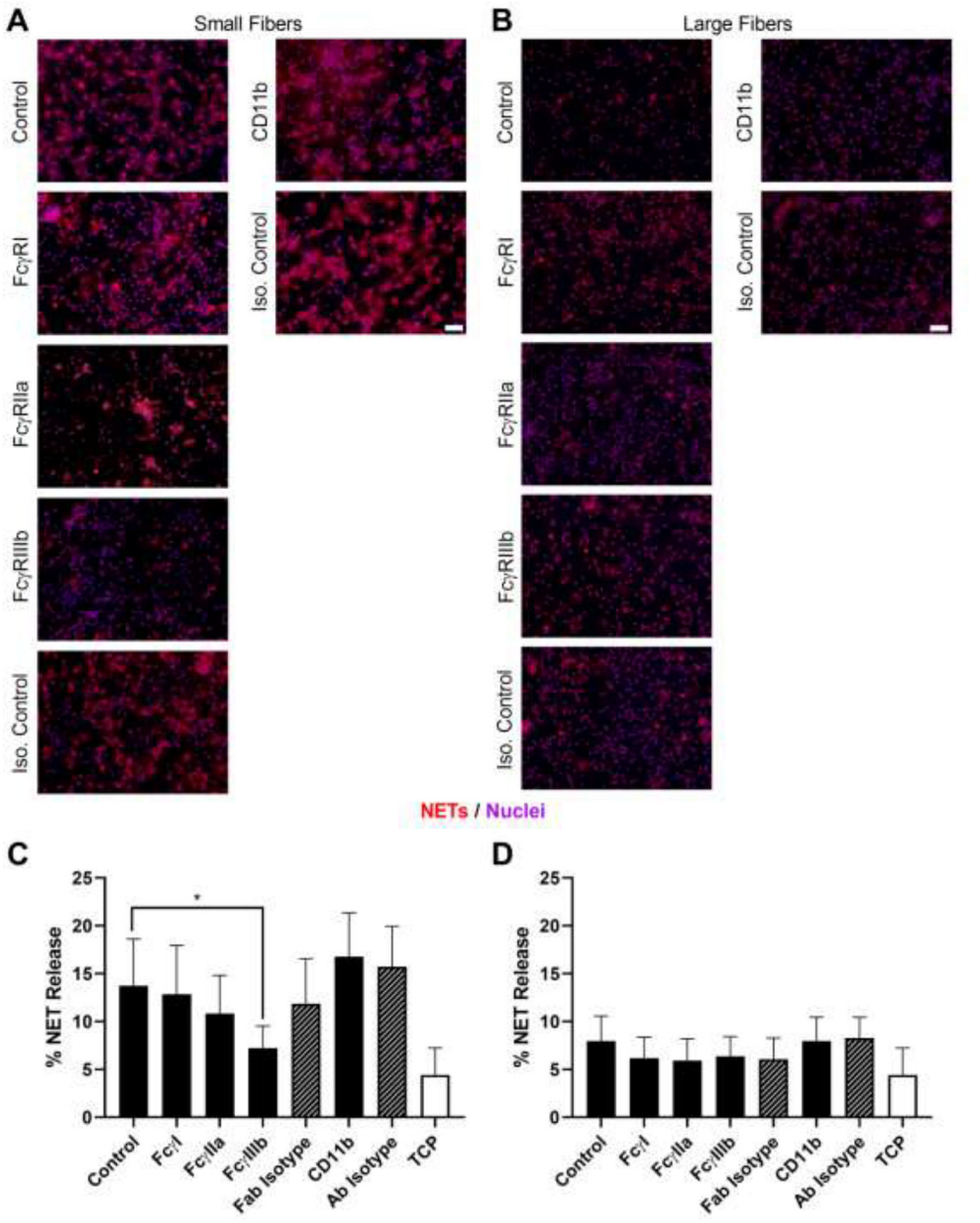

Figure 4.

Blocking FcγIIIb decreases biomaterial-induced NET release on small but not large fiber biomaterials. (A and B) Fluorescent micrographs of neutrophils on the electrospun biomaterials at 3 hours after seeding. NETs are shown in red and nuclei in purple. Scale bars are 50 μm. (C and D) Percent NET release at 3 hours as quantified by the ELISA for NET-disassociated MPO. The quantification of percent NET release (n = 4) indicates that blocking FcγIIIb on the small fiber biomaterials significantly reduces NET formation whereas no effect is observed on the large fiber biomaterials. The data represent the mean ± standard deviation of three independent experiments with unique donors. * $p < 0.05$ was determined using an ANOVA and Holm-Sidak's multiple comparisons test. Raw data is available in Supplementary Spreadsheet 1.

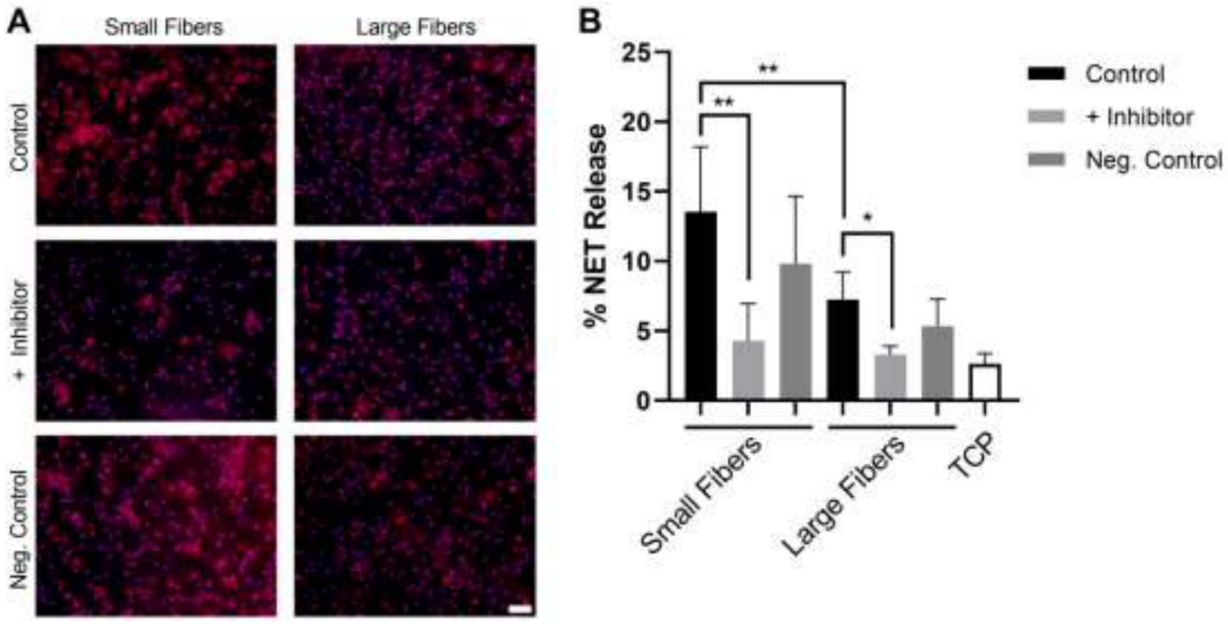

Figure 5.

Inhibition of FcγIIIb signaling through TAKI attenuates NET release on both small and large fiber biomaterials. (A) Fluorescent micrographs of neutrophils on the electrospun biomaterials at 3 hours after seeding. NETs are shown in red and nuclei in purple. The scale bar is 50 μm. (B) Percent NET release at 3 hours as quantified by the ELISA for NET-disassociated MPO. The quantification of percent NET release (n = 6) indicates that inhibition of TAKI reduces NET formation on both the small and large fiber electrospun biomaterials. The data represent the mean ± standard deviation of three independent experiments with unique donors. * $p < 0.05$ and ** $p < 0.0001$ were determined using an ANOVA and Holm-Sidak's multiple comparisons test. Raw data is available in Supplementary Spreadsheet 1.

Table 1.

Electrospun biomaterials were fabricated with optimized parameters.

Fiber Size	PDO Concentration (mg/mL)	Flow Rate (mL/h)	Airgap Distance (cm)	Applied Voltage (+ kV)
Small Fibers	50	0.55	28	25
Large Fibers	120	4.0	28	28